ESI

Fluorescent supramolecular hierarchical self-assemblies from glycosylated 4-amino- and 4-bromo-1,8-naphthalimides

Elena Calatrava-Pérez, [a] Stefan Acherman, [a] Lucas Stricker, [a] Gavin McManus,[b] Jason Delente, [a] Amy D. Lynes, [a] Adam F. Henwood, [a] June I. Lovitt, [a] Chris S. Hawes, [a] Kevin Byrne, [a] Wolfgang Schmitt, [a] Oxana Kotova, [a] Thorfinnur Gunnlaugsson[a]* and Eoin M. Scanlan[a]

Synthesis:

N-Propargyl-4-bromo-1,8-naphthalimide[1]

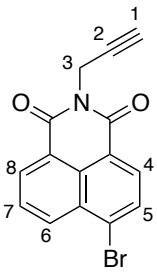

2-Propyn-1-amine (0.14 mL, 2.16 mmol, 1.20 equiv) was added to a solution of 4-bromo-1,8-naphthalic anhydride (0.50 g, 1.80 mmol, 1.00 equiv) in ethanol (20 mL). After 3 h refluxing, the reaction was dried *in vacuo* to afford the product **105** as a brown powder (0.56 g, 99%). $\mathbf{R_f}$. = 0.5 (2:3 (v/v), EtOAc:Hex).

$\boldsymbol{\delta_H}$ (400 MHz, $CDCl_3$): 8.70 (dd, $J_{8\text{-}7}$ = 7.3 Hz, $J_{8\text{-}6}$ = 1.1 Hz, 1H, H-8), 8.60 (dd, $J_{6\text{-}7}$ = 8.5 Hz, $J_{6\text{-}8}$ = 1.1 Hz, 1H, H-6), 8.46 (d, $J_{4\text{-}5}$ = 7.9 Hz, 1H, H-4), 8.06 (d, $J_{5\text{-}4}$ = 7.9 Hz, 1H, H-5), 7.87 (dd, J = 8.5, 7.3 Hz, 1H, H-7), 4.95 (d, $J_{2\text{-}1}$ = 2.5 Hz, 2H, H-3), 2.20 (t, $J_{1\text{-}2}$ = 2.5 Hz, 1H, H-1). **HRMS** (*m/z* - ESI^+): Found: 313.98254 ($[M+H]^+$, $C_{15}H_9BrNO_2$ Required: 313.98111).

General Procedure for the Synthesis of 1,[2] 2[2] and 3 (see below)

The corresponding alkyne derivative (1.1 equiv) and tetrakis(acetonitrile)-copper(I)tetrafluoroborate ($[(CH_3CN)_4Cu]BF_4$) (0.15 eq.) were added to a solution of the corresponding azide (1 equiv) in DMF (5 mL) in a microwave vial. The reaction mixture was stirred for 1 h at 115 °C in a microwave reactor. The solvent was removed *in vacuo* and the crude product dissolved in a mixture of $MeOH/CH_2Cl_2$ (1:2) and filtered through a plug of Celite® to remove the copper catalyst. The filtrate was concentrated *in vacuo* and purified by SiO_2 column chromatography, previously base treated with Et_3N, using 20-30% MeOH/EtOH (v/v), to afford the corresponding product.

N-((1-(3-(β-D-galactopyranosyloxy)propyl)-1H-1,2,3-triazol-4-yl)methyl)-4-bromo-1,8-naphthalimide (3)

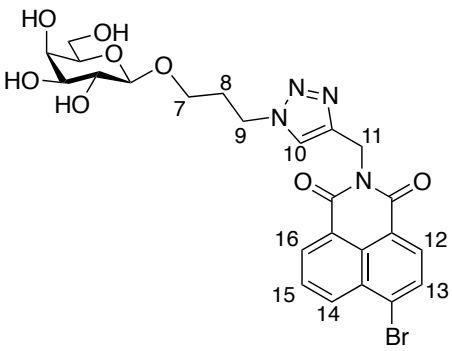

Following general procedure D: 1-O-(3-azidopropyl)-β-D-galactopyranoside (0.28 g, 1.06 mmol, 1.3 equiv), and *N*-propargyl-4-bromo-1,8-naphthalimide (0.256 g, 0.818 mmol, 1.0 equiv), $[(CH_3CN)_4Cu]BF_4$ (38.00 mg, 0.12 mmol, 0.15 mmol) and DMF (15 mL) were used. Product **3** was afforded as an orange powder (0.46 g, 98%). $\mathbf{R_f}$. = 0.20 (1:1 (v/v), EtOAc/Hex)

$\boldsymbol{[\alpha]_D^{20}}$ = 20 deg cm^3 g^{-1} dm^{-1} (0.1, MeOH). $\boldsymbol{\delta_H}$ (400 MHz, DMSO): 8.59 (app t, 2H, H-14, H-16), 8.36 (d, $J_{12\text{-}13}$ = 7.9

Hz, 1H, H-12), 8.24 (d, $J_{13\text{-}12}$ = 7.9 Hz, 1H, H-13), 8.05 – 7.98 (m, 1H, H-15, DMF), 7.93 (s, 1H, H-10), 5.28 (s, 2H, H-11), 4.85 (d, *J* = 4.6 Hz, 1H, OH), 4.61 (d, *J* = 5.6 Hz, 1H, OH), 4.50 (app t, 1H, OH), 4.38 (app t, 2H, H-9), 4.30 (d, *J* = 4.6 Hz, 1H, OH), 4.03 – 3.96 (m, 2H, H-1, OH), 3.70 (dt, *J* = 11.1, 5.8 Hz, 1H, H-6), 3.57 (t, *J* = 4.1 Hz, 1H), 3.52 – 3.38 (m, 2H, H-7), 3.19 – 3.11 (m, 3H), 2.04 – 1.93 (m, 2H, H-8). **δ_C** (100 MHz, DMSO): 133.3 (q, C-16), 132.4 (q, C-15), 131.6 (q, C-13), 131.5 (q, C-12), 129.0 (q, C-14), 104.5 (C-1), 73.5, 70.9, 68.5, 65.4 (C-6), 61.07 (C-7), 47.9 (C-8), 35.7 (C-11), 30.3 (C-8). **ν_{max}** (ATR)/cm^{-1}: 3354 (OH), 2923, 1702, 1661 (C=O), 1587 (ar. C-C), 1368, 1344, 1235, 1055., 1033, 953, 783, 577. **HRMS** (*m/z* - ESI^+): Found: 599.073311, ($[M+Na]^+$. $C_{24}H_{25}BrN_4NaO_8$, Required: 599.074797)

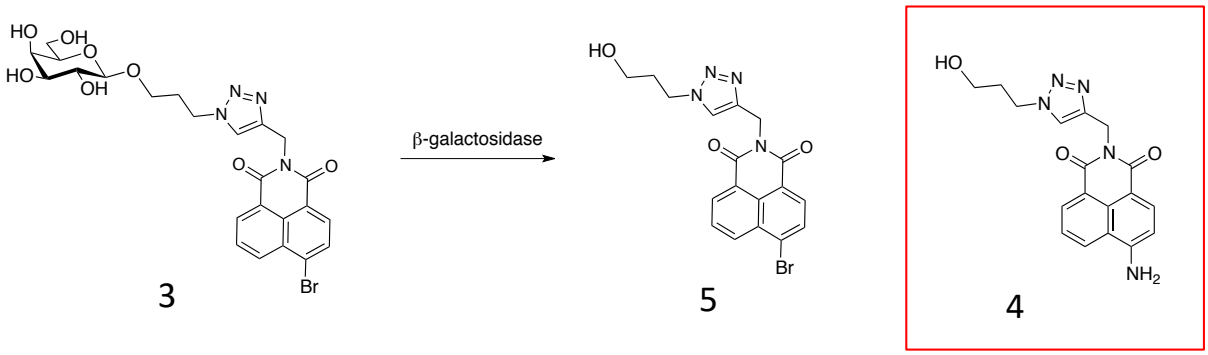

Scheme S1. Enzymatic hydrolysis of compound **3** to give compound **5** upon treatment with β-galactosidase enzyme (1 U) in PBS (pH 7.2) at 30 °C for 16 h. The final product **4**, from **1** and **2** is also shown. Compound **5** was not characterised by NMR studies upon enzymatic cleavage due to low concentration.

Enzymatic Activity Evaluation

The changes in the absorption and emission spectra over time after the addition of galactosidase were next examined at pH 7.2 and 30 °C (optimal conditions for this enzyme). For compound **1**, which gave **4** above, enzymatic hydrolysis did not lead to a significant change in the ICT absorption or fluorescence emission over time. Different concentrations of the enzyme (0.01, 0.1 and 1.0 U) were added to the solution, and the same behaviour was observed. Importantly, no significant changes were seen in the absorption spectra of upon addition of enzymes, which rules out any non-specific or strong association between the enzyme and the naphthalimide substrate.

Figures:

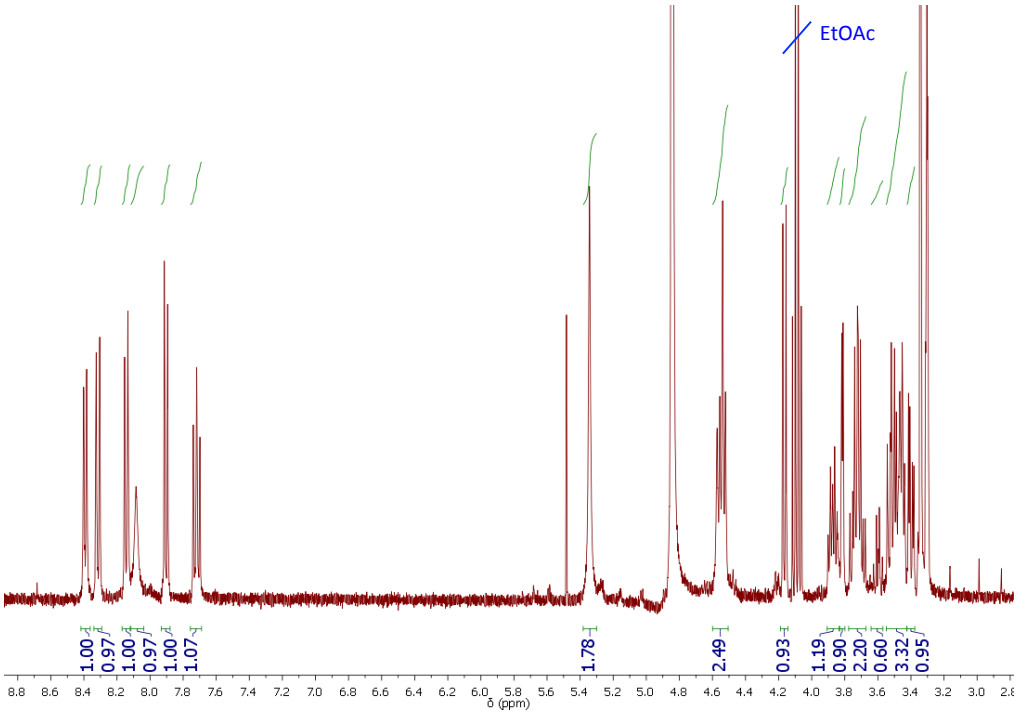

Figure S1. The ^{1}H NMR (400 MHz) of compound **3** in CD_3OD.

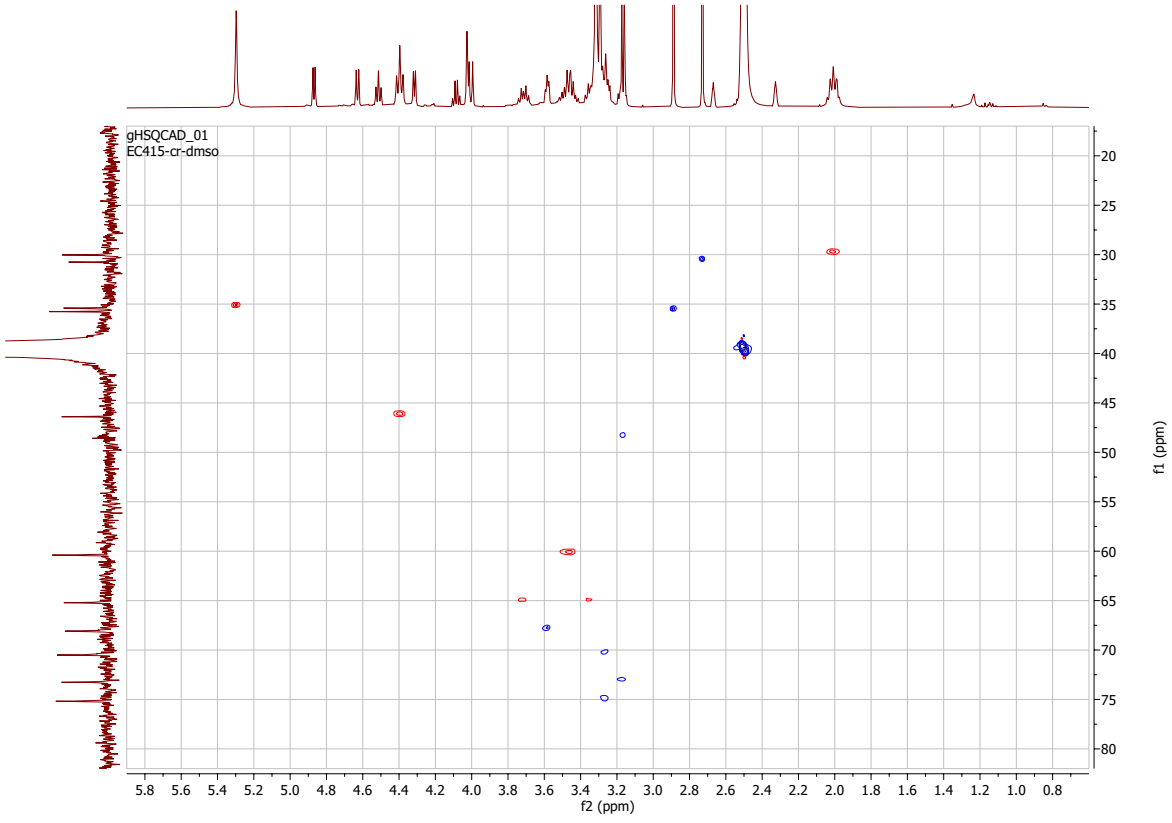

Figure S2. HSQC NMR of compound **3**.

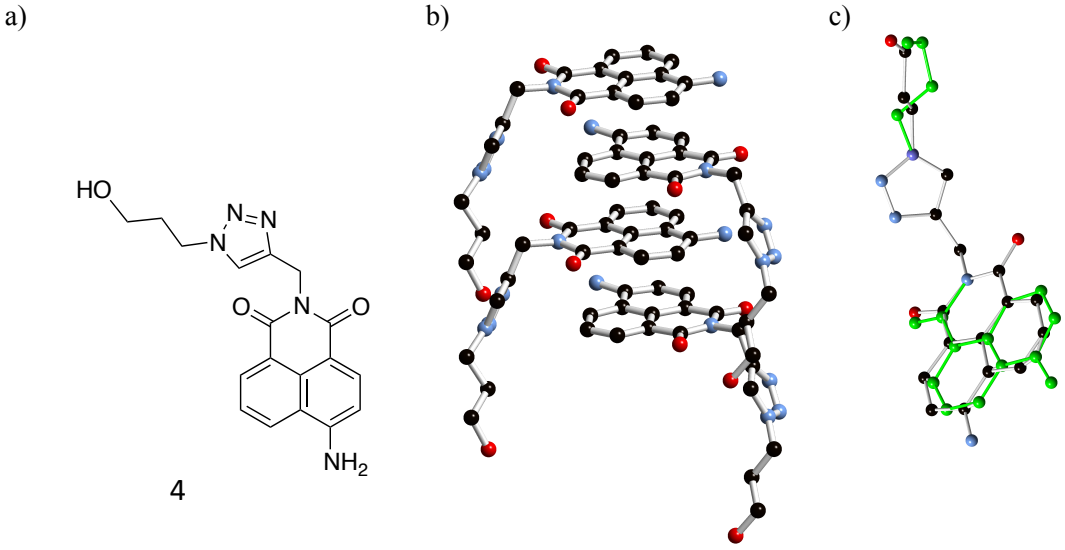

Figure S3 a) Chemical structure of compound **4** and its X-ray crystal structure formed in H_2O showing its π–π interactions (b) and two disordered orientations of the molecules (c). The crystal structure is reproduced from our previous work published in OBC in 2019.[3]

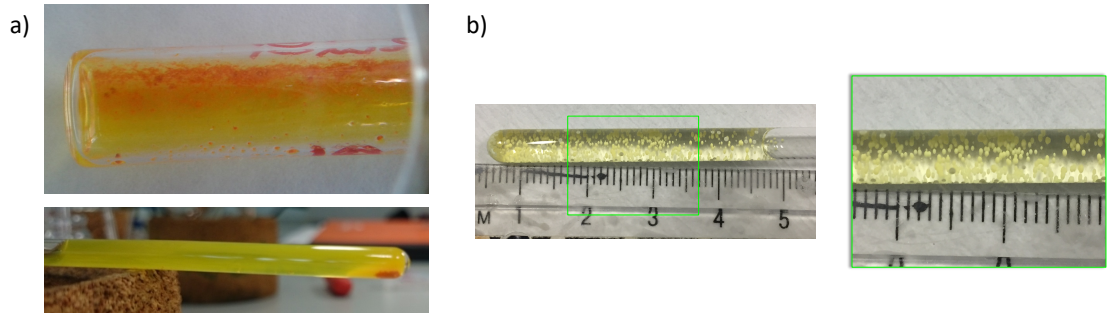

Figure S4 a) Microspheres of compound **1** in methanol (top) and deutrated methanol (bottom). b) Aggregates formed by compound **3** in CD_3OD.

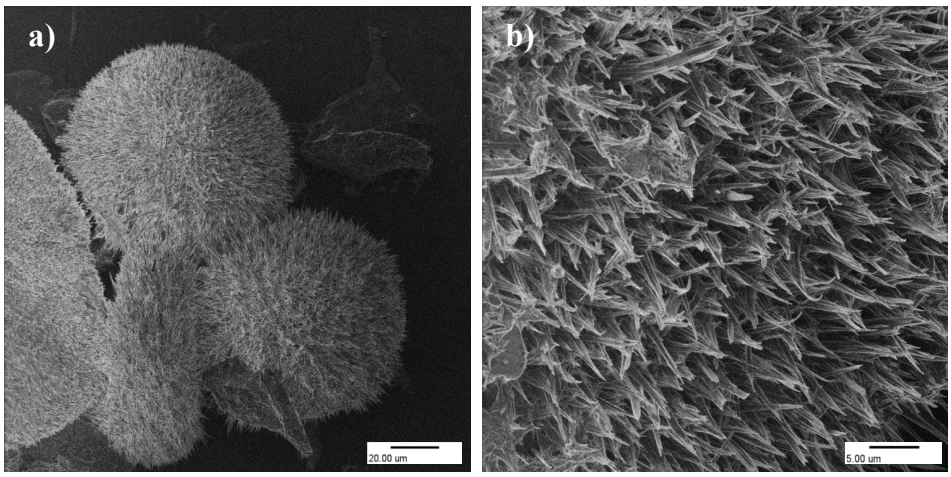

Figure S5 a) HIB images of **1** based particles that were reproduced and imaged using a freshly made batch of **1**.

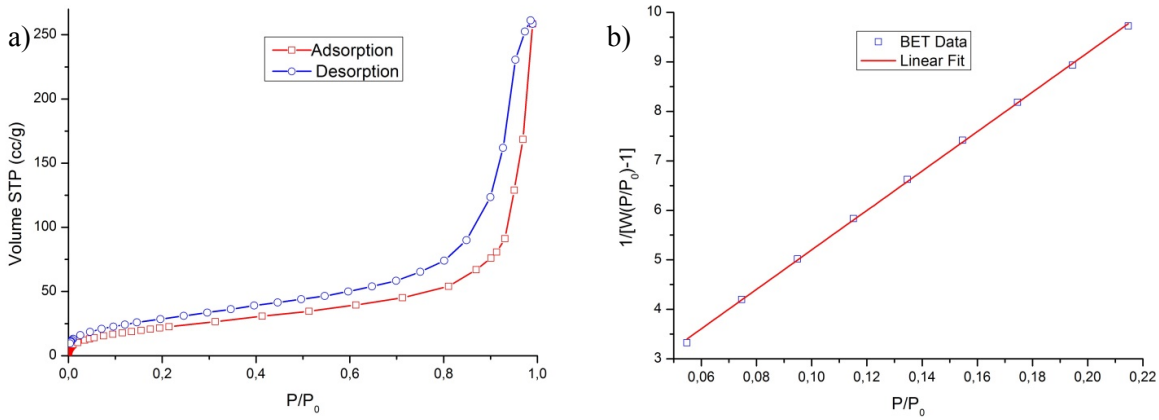

Figure S6 a) Surface measurement of microsphares formed from compound **1**. a) Adsorption/desorption isotherm and b) BET plot and linear fit.

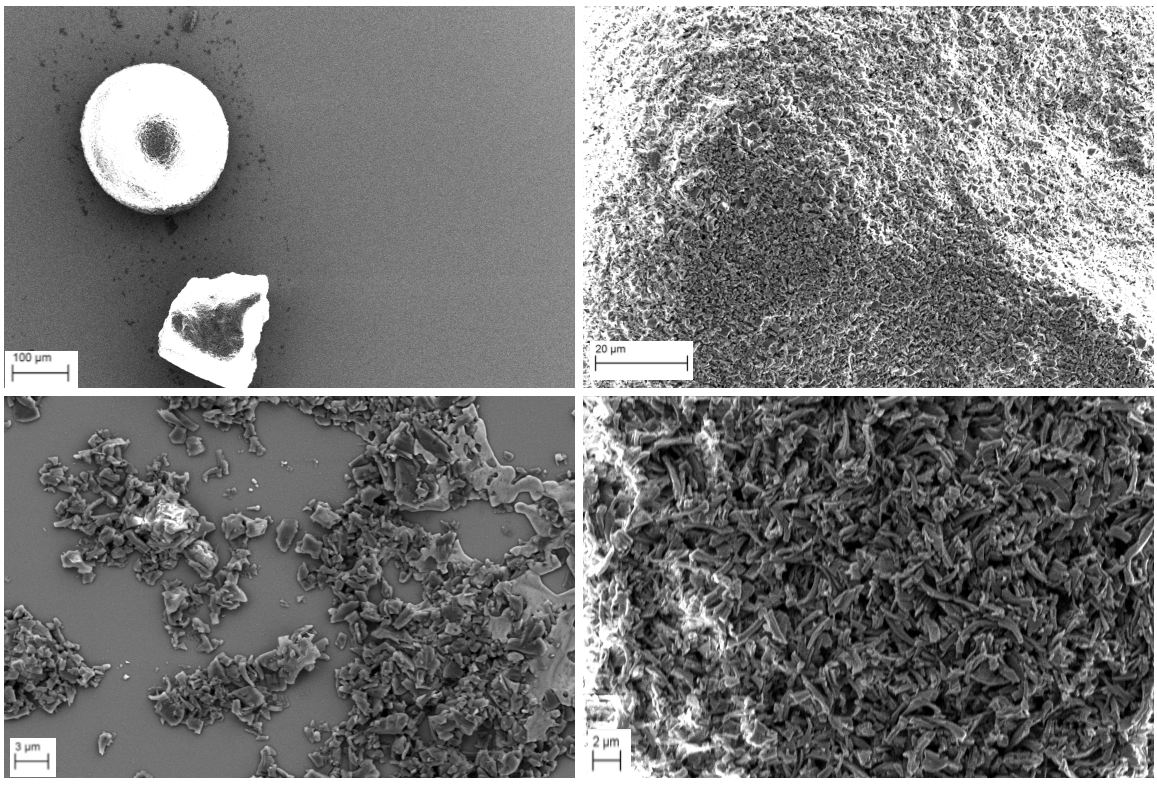

Figure S7 a) SEM images of aggregates formed by compound **2** in CD_3OD.

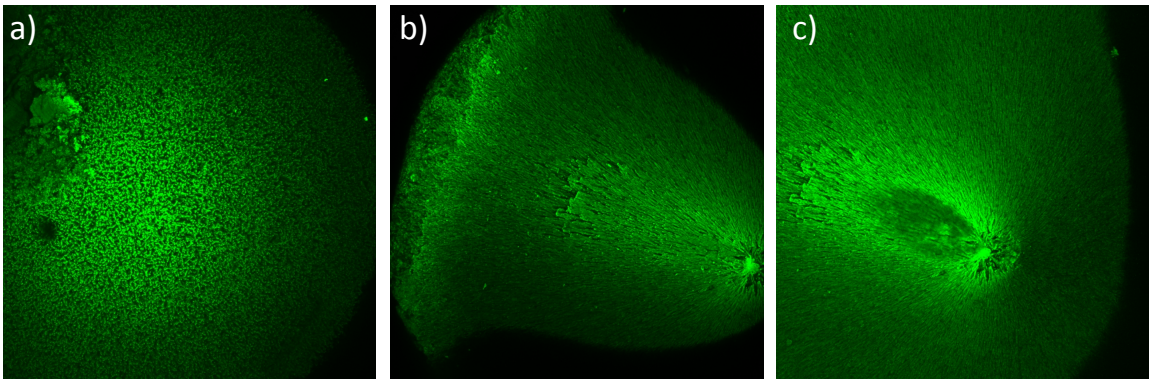

Figure S8. Confocal fluorescence microscopy images of a new batch of compound **3** showing the (reproduction of the) formation of spherical aggregates in CD_3OD.

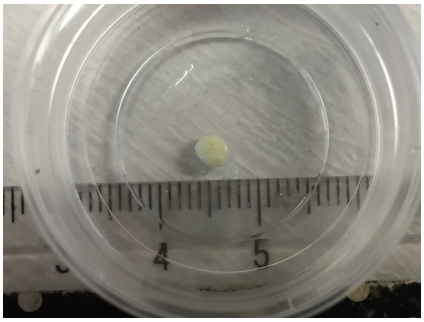

Figure S9. Sphere formed by compound **3** in PBS after being dried overnight at rt.

X-ray Crystallography

Structural and refinement parameters are presented in Table S1. All diffraction data was measured using a Bruker APEX-II Duo dual-source instrument using a microfocus Cu Kα (1.5405 Å) radiation as specified. Datasets were collected using ω and ϕ scans with the samples immersed in NVH immersion oil and maintained at a constant temperature of 100 K using a Cobra cryostream. The data was reduced and processed using the Bruker APEX-3 suite of programs.[4] Multi-scan absorption corrections were applied using SADABS.[5] The diffraction data were solved using SHELXT and refined by full-matrix least squares procedures using SHELXL-2015 within the OLEX-2 GUI.[6,7] All non-hydrogen atoms were refined with anisotropic displacement parameters. All carbon-bound hydrogen atoms were placed in calculated positions and refined with a riding model, with isotropic displacement parameters equal to either 1.2 or 1.5 times the isotropic equivalent of their carrier atoms. CCDC 1968851- 1968853.

Crystals of compound **6** exhibited poor diffraction characteristics with generally low intensity scattering and no useful reflections beyond 0.98 Å resolution. Therefore, the structure model presented for compound **6** is purely a connectivity model presented only to support the conclusions drawn from supporting characterisation methods.

For all three 4-bromonaphthalimide structures, the bromine atom is disordered over two positions, essentially related by a rotation of the entire naphthalimide group about the N_{imide}-CH_2 bond with a slight rotation about the vector normal to the aromatic plane. Similar disorder modes are regularly observed in 4-monosubstituted 1,8-naphthalimides (Figure S3). Because of the large contribution of the bromine position to the scattering factors, these positions (less than 10% occupancy) can be readily detected for this atom, but the 12 associated low-occupancy carbon positions could not be reasonably modelled due to the overlap with the primary contributor. As such, the bromine sites are modelled as isolated atoms for the second geometry and are not intended to represent a sensible molecular geometry in connection with the modelled carbon positions. The disorder ratios (free variable refinement) are approximately 95:5 ratio for **6**, and approximately 93:7 for **7** and **8**. The structure of **7** was previously reported by Goudappagouda as a room temperature dataset.[9]

Table A1: Crystallographic and refinement parameters for all structures

Identification code	**6**	**7**	**8**
Empirical formula	$C_{14}H_{10}BrNO_2$	$C_{32}H_{28}Br_2N_2O_4$	$C_{20}H_{22}BrNO_2$
Formula weight	304.14	664.38	388.29
Temperature/K	100(2)	100(2)	100(2)
Crystal system	monoclinic	triclinic	triclinic
Space group	$P2_1/c$	P-1	P-1
a/Å	13.7872(9)	4.4247(3)	4.6972(2)
b/Å	11.4491(7)	16.1174(10)	11.9618(5)
c/Å	7.3967(5)	19.4957(13)	15.7954(7)
α/°	90	99.692(2)	81.534(3)
β/°	101.273(3)	94.484(2)	86.654(4)
γ/°	90	92.775(2)	84.890(3)
Volume/Å^3	1145.05(13)	1363.61(16)	873.41(7)
Z	4	2	2
ρ_{calc}g/cm^3	1.764	1.618	1.476
μ/mm^{-1}	4.837	4.115	3.296
F(000)	608.0	672.0	400.0
Crystal size/mm^3	0.2 × 0.11 × 0.05	0.18 × 0.06 × 0.02	0.14 × 0.08 × 0.02
Radiation	CuKα (λ = 1.54178)	CuKα (λ = 1.54178)	CuKα (λ = 1.54178)
2Θ range for data collection/°	6.536 to 103.702	5.574 to 136.426	7.496 to 136.638
Index ranges	-14 ≤ h ≤ 14, -11 ≤ k ≤ 11, -7 ≤ l ≤ 7	-5 ≤ h ≤ 5, -15 ≤ k ≤ 18, -23 ≤ l ≤ 23	-5 ≤ h ≤ 5, -14 ≤ k ≤ 11, -18 ≤ l ≤ 18
Reflections collected	10189	12740	7358
Independent reflections	1274 [R_{int} = 0.0771, R_{sigma} = 0.0387]	4955 [R_{int} = 0.0299, R_{sigma} = 0.0346]	3139 [R_{int} = 0.0449, R_{sigma} = 0.0565
Data/restraints/parameters	1274/0/164	4955/2/376	3139/0/227
Goodness-of-fit on F^2	1.179	1.098	1.136
Final R indexes [I>=2σ (I)]	R_1 = 0.0957, wR_2 = 0.2070	R_1 = 0.0410, wR_2 = 0.1059	R_1 = 0.0732, wR_2 = 0.1867
Final R indexes [all data]	R_1 = 0.1040, wR_2 = 0.2110	R_1 = 0.0420, wR_2 = 0.1066	R_1 = 0.0839, wR_2 = 0.1935
Largest diff. peak/hole / e Å^{-3}	1.94/-0.69	0.96/-0.81	1.24/-0.61
CCDC No.	1968851	1968852	1968853

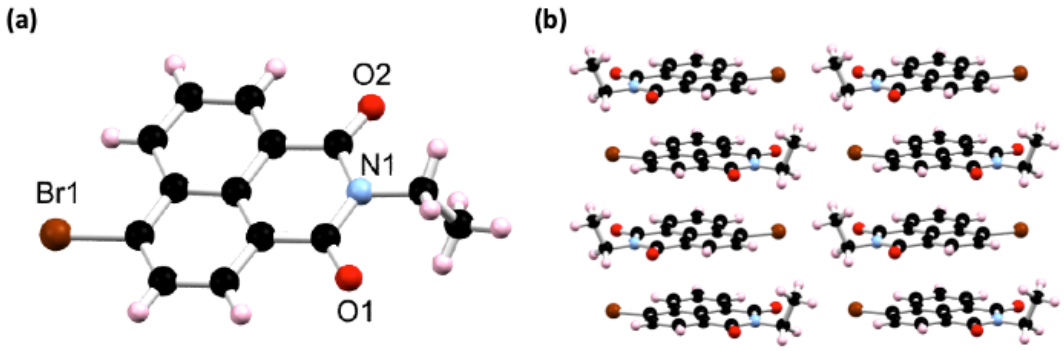

Figure S10 a) The structure of compound **6** with heteroatom labelling scheme. **(b)** illustrates the side on view of offset head to tail π-π stacking within the extended structure between adjacent naphthalimide groups.

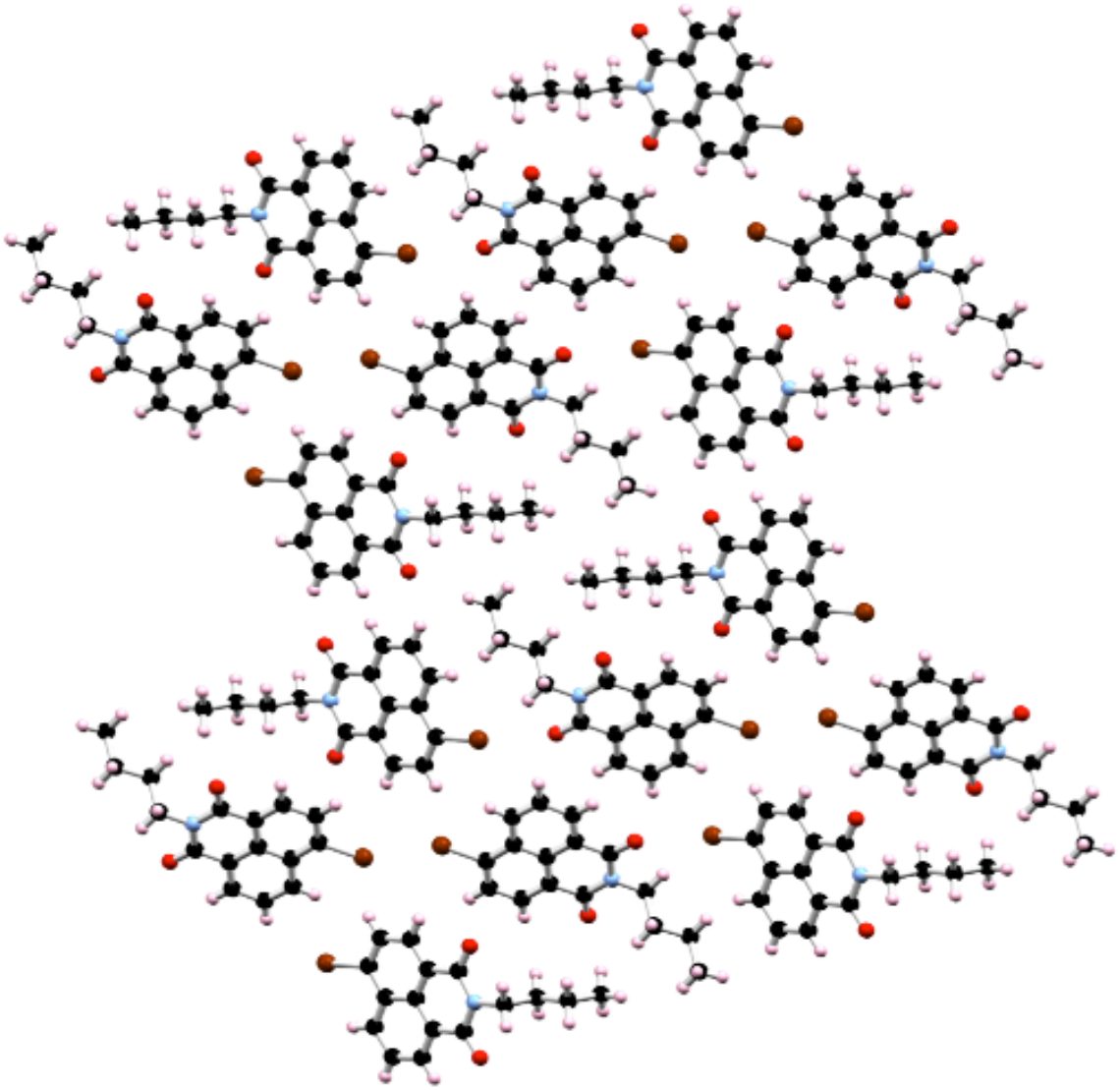

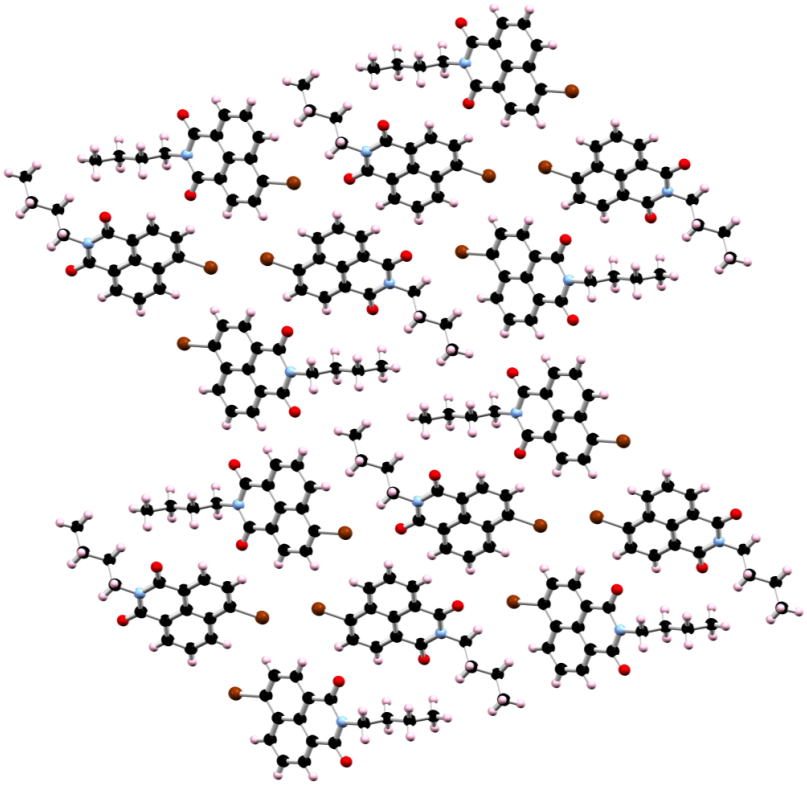

Figure S11) The offset head to tail π-π stacking within the extended structure of compound **6** between adjacent naphthalimide groups.

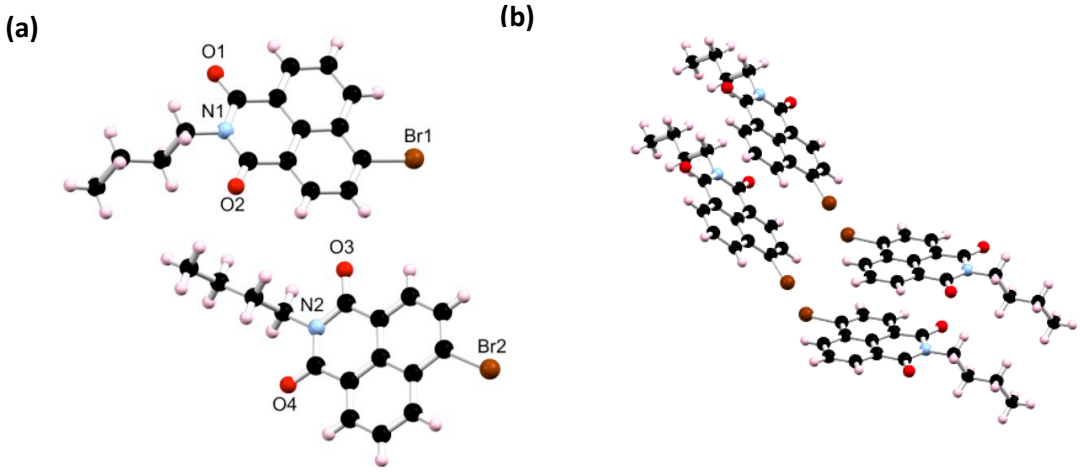

Figure S12 a) The structure of compound **7** with heteroatom labelling scheme. **(b)** illustrates the side-on view of offset face to face π-π stacking within the extended structure between adjacent naphthalimide groups. The structure is analogous to the contemporary report by Goudappagouda;[9] the low-temperature structure is reported here for posterity.

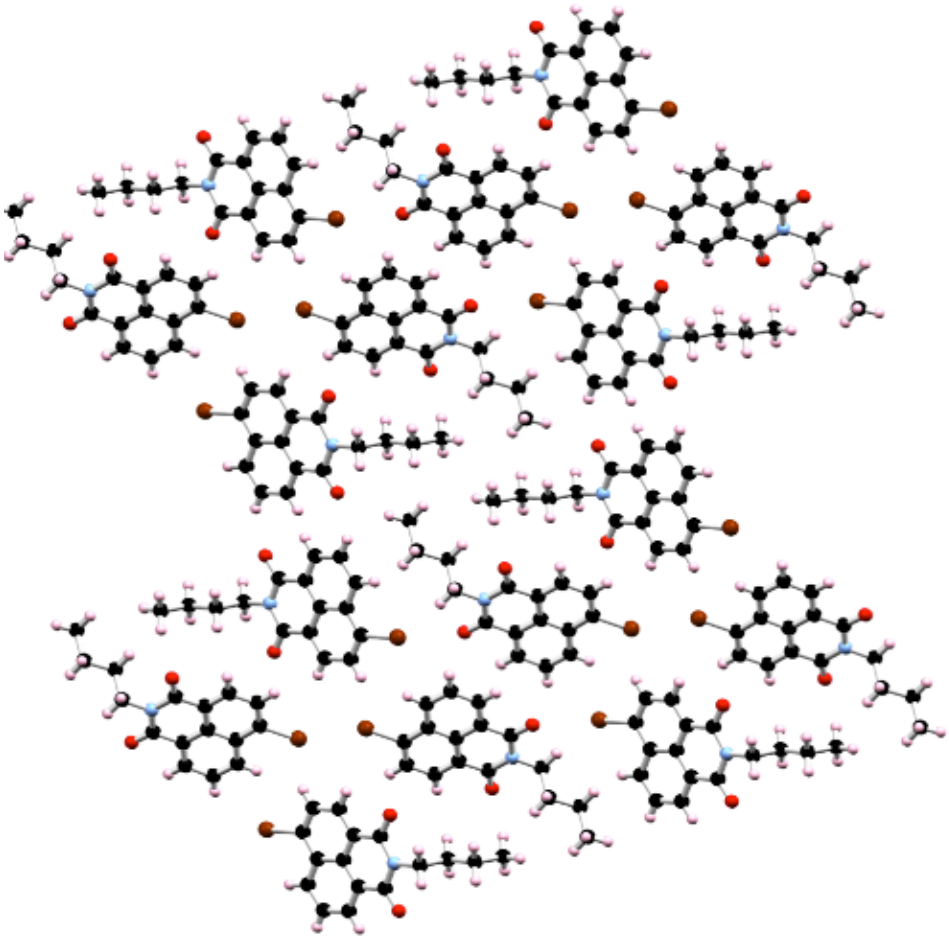

Figure S13) The offset face to face π-π stacking within the extended structure of compound **7** between adjacent naphthalimide groups.

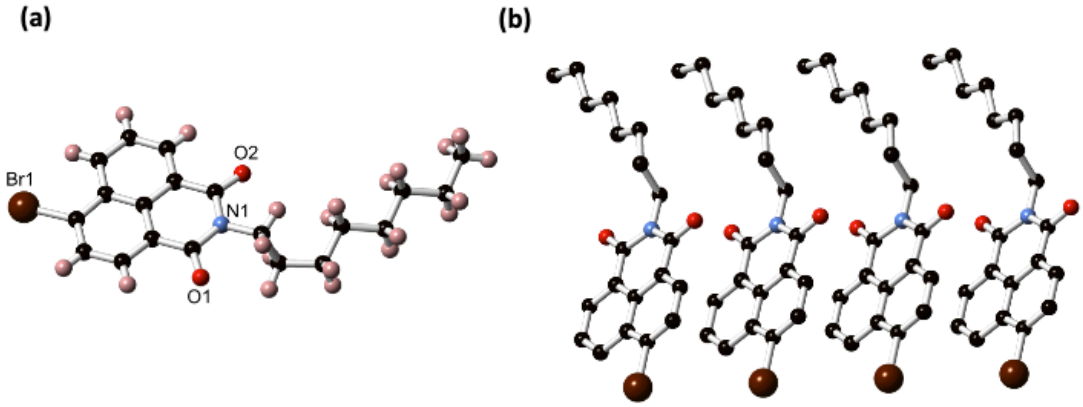

Figure S14 a) The structure of compound **8** with heteroatom labelling scheme. **(b)** illustrates the side-on view of offset face to face π-π stacking within the extended structure between adjacent naphthalimide groups. Hydrogen atoms omitted for clarity.

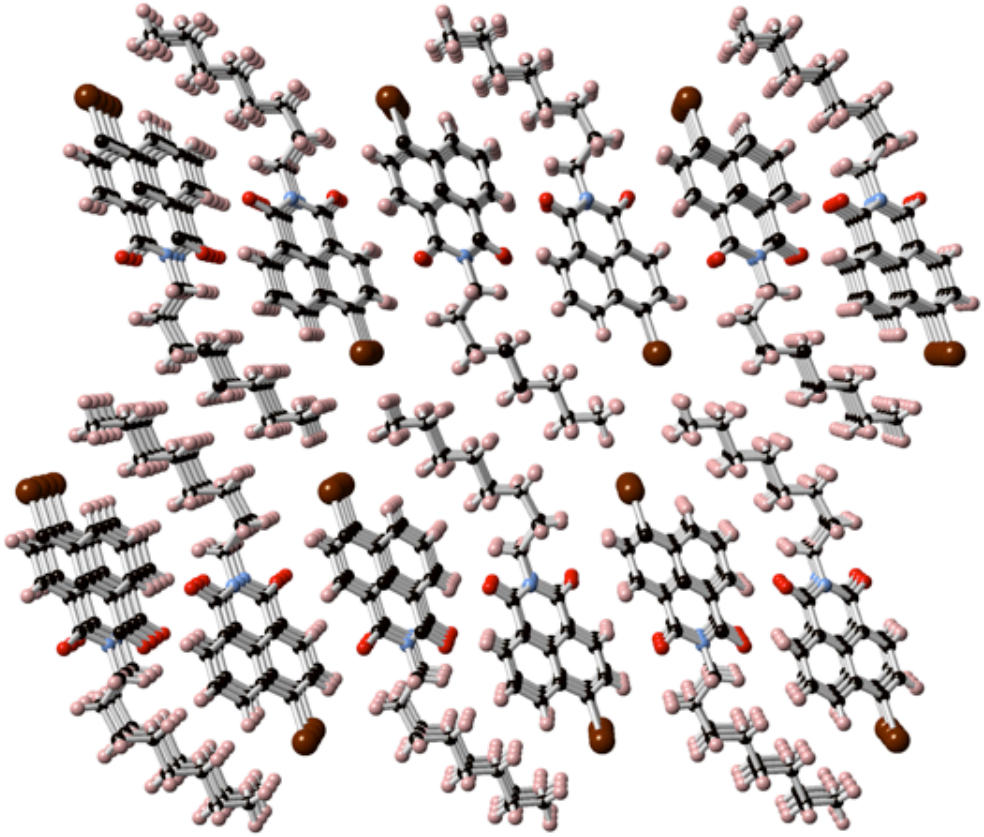

Figure S15 a) The offset face to face π-π stacking within the extended structure of compound **8** between adjacent naphthalimide groups.

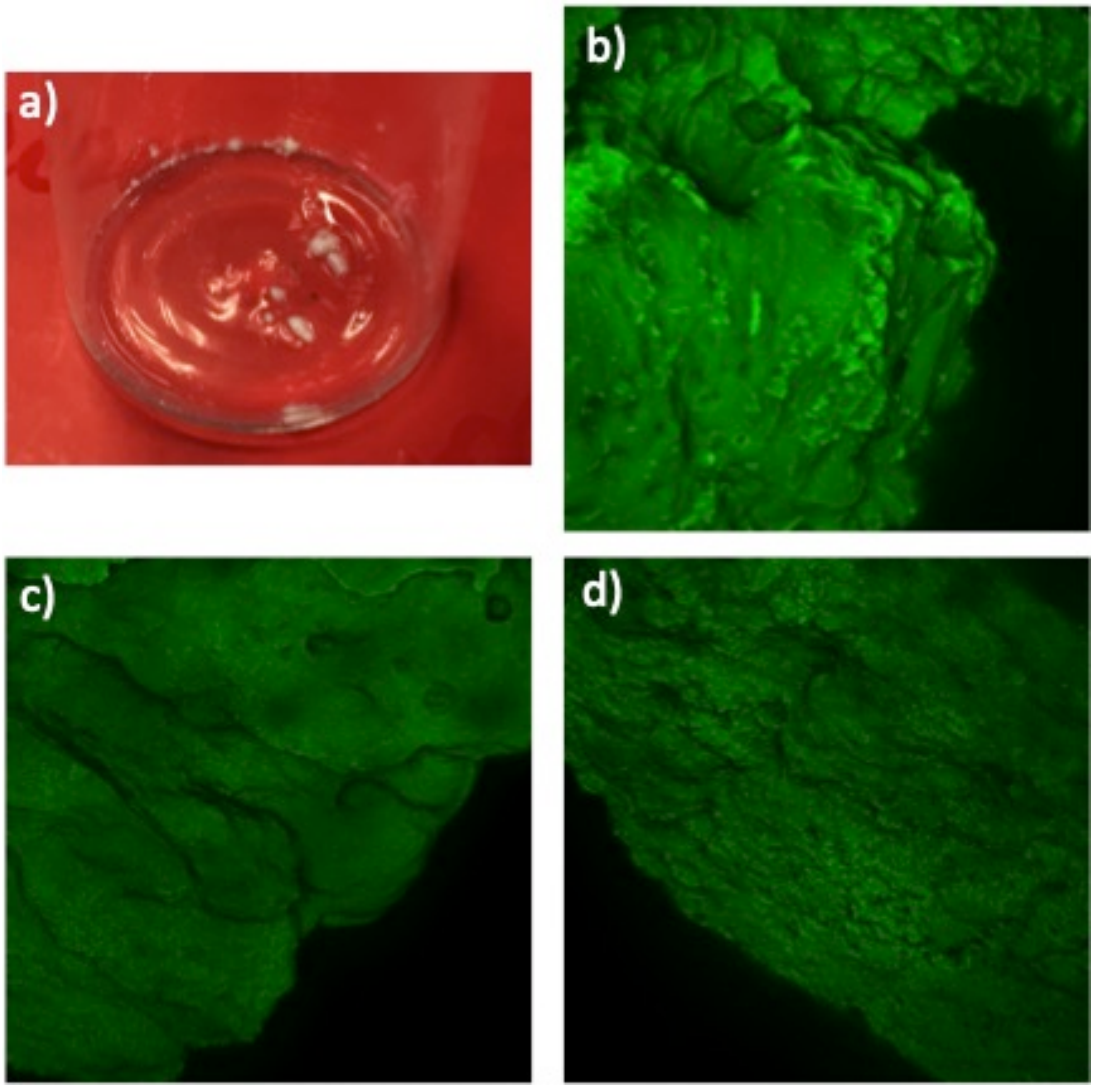

Figure S16. a) Image and b-d) confocal fluorescence microscopy images of compound **3** after treatment with 1 U β-galactosidase for 16 h at 30 °C

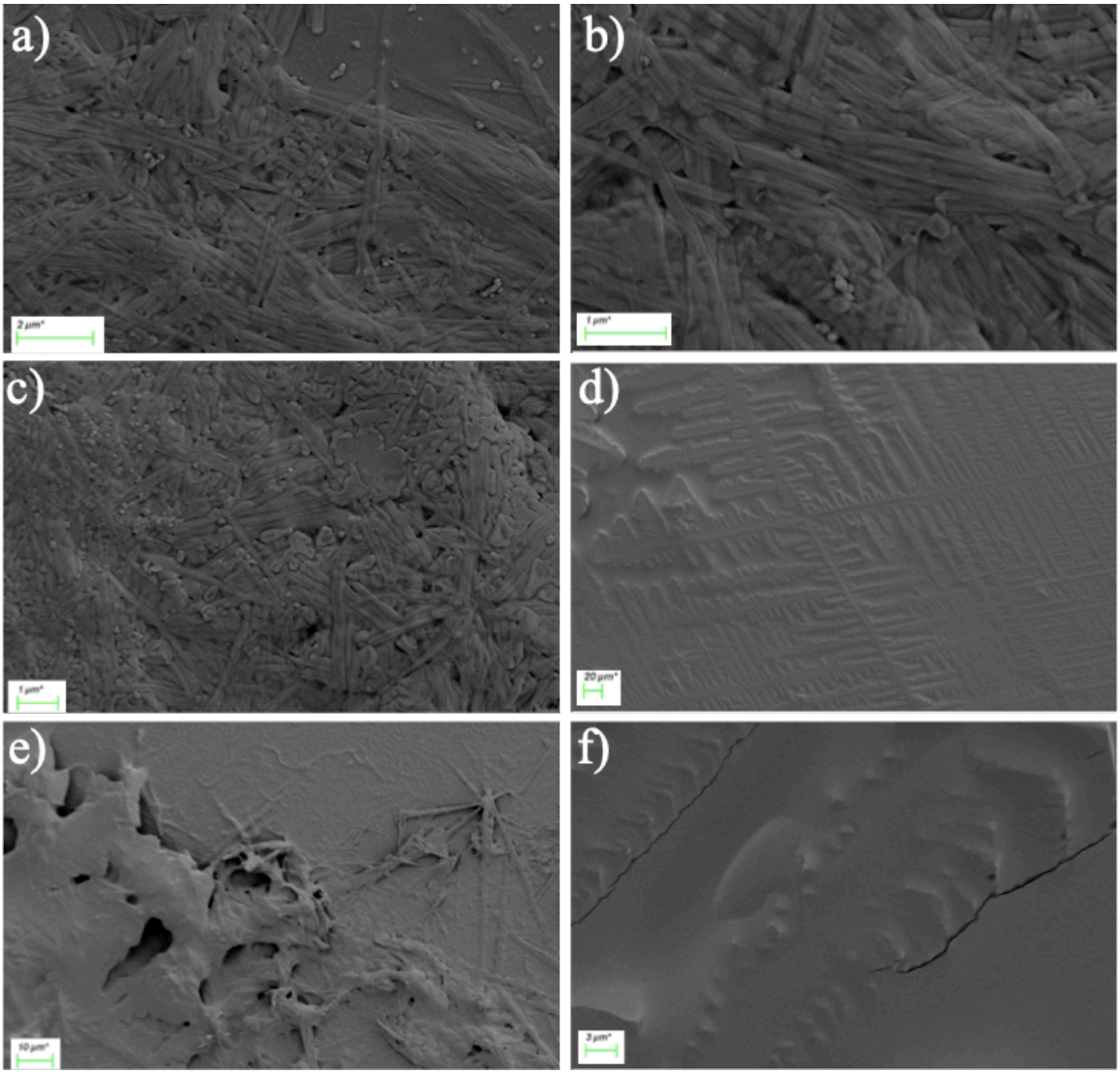

Figure S17. SEM images of compound **3** in PBS before (a-c) and after treatment with 1 U of β-galactosidase for 16 h (d-f).

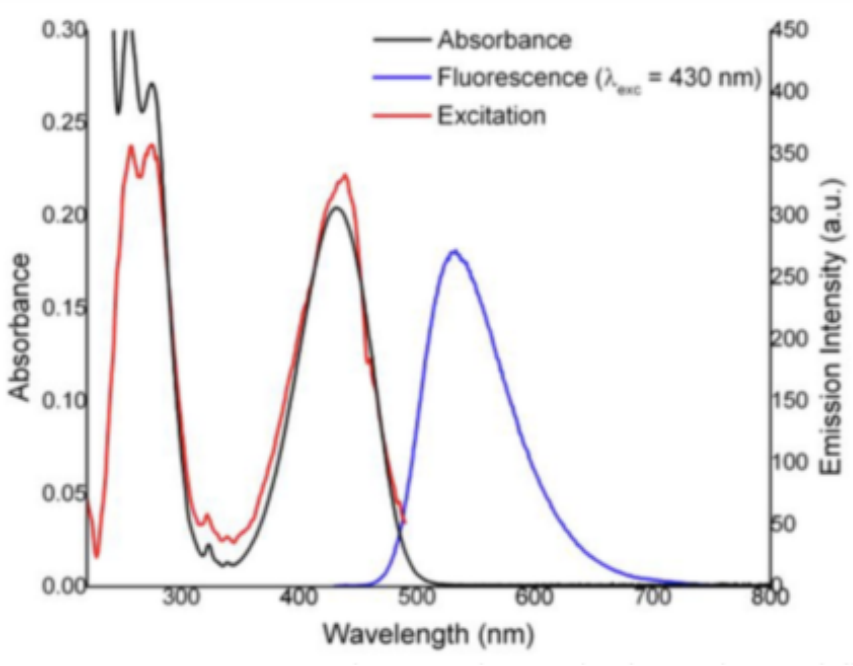

Figure 18. The UV Vis and fluorescnece emission absorption spectrum of **1**.

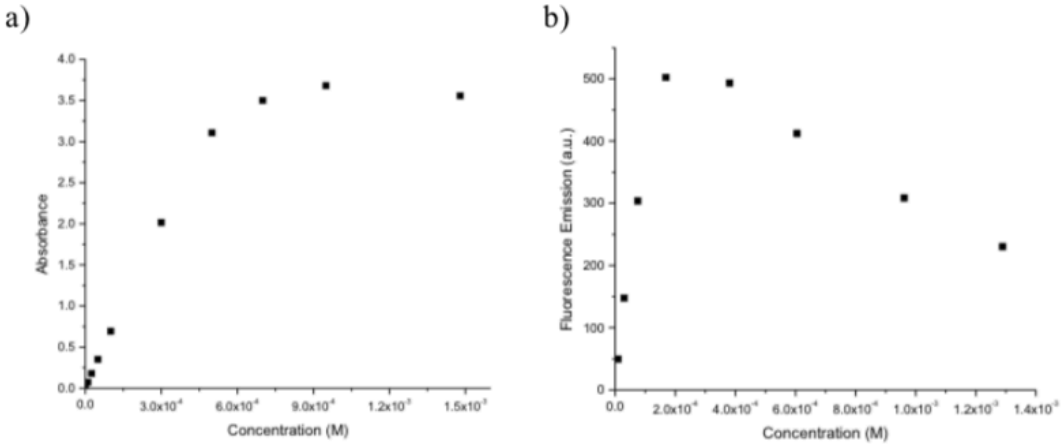

Figure 19. Changes in a) absorbance and b) fluorescence spectra (max = 430 nm) of compound **1** in 10 mM PBS pH 7.2 with respect to concentration. All the measurements were recorded at rt. Experiment carried out twice.

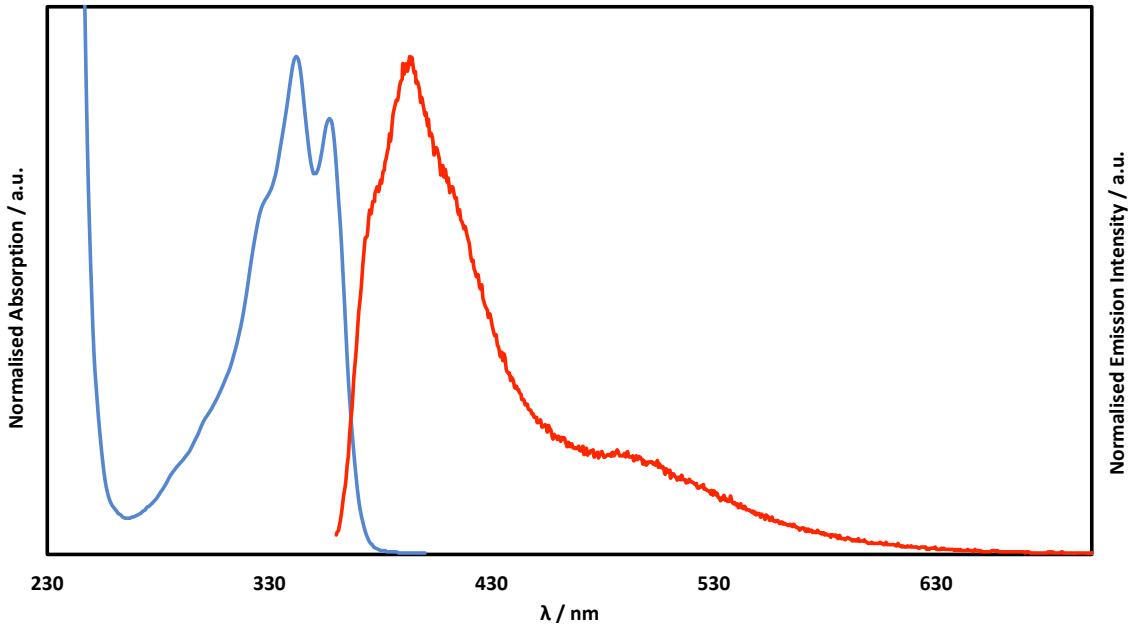

Figure 20. The absorbance and fluorescence spectra of 4-Br NAp at rt and 5.15 x 10^{-5} M concentraions in MeOH.

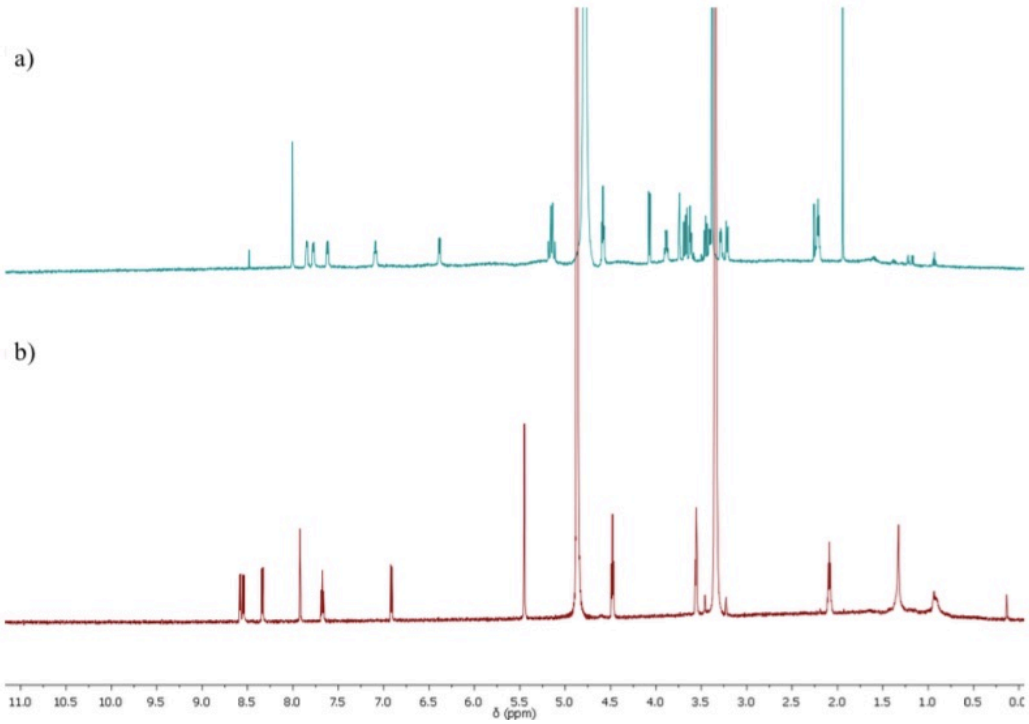

Figure 21. ^{1}H NMR (600 MHz) of a) compound **1** recorded in D_2O and b) **4** recorded in CD_3OD.

References:

1. J. Pancholi, D. J. Hodson, K. Jobe, G. A. Rutter, S. M. Goldup, M. Watkinson, *Chem. Sci.* 2014, **5**, 3528-3535.
2. E. Calatrava-Perez, S. A. Bright, S. Achermann, C. Moylan, M. O. Senge, E. B. Veale, D. C. Williams, T. Gunnlaugsson and E. M. Scanlan, *Chem. Commun.*, 2016, **52**, 13086-13089.
3. E. Calatrava-Pérez, J. M. Delente, S. Shanmugaraju, C. S. Hawes, C. D. Williams, T. Gunnlaugsson, and E. M. Scanlan, *Org. Biomol. Chem*., 2019, **17**, 2116–2125
4. *Bruker APEX-3*, Bruker-AXS Inc., Madison, WI, 2016.
5. *SADABS*, Bruker-AXS Inc., Madison, WI, 2016.
6. Sheldrick, G. M. *Acta Crystallogr. Sect. A.* **2015**, *71*, 3-8.
7. Sheldrick, G. M. *Acta Crystallogr. Sect. C.* **2015**, *71*, 3-8.
8. A. L. Spek, *Acta Crystallogr. Sect. C.,* 2015, **71**, 9-18.
9. A. M. Goudappagouda, V. C. Wakchaure, K. C. Ranjeesh, T. Das, K. Vanka, T. Nakanishi and S. S. Babu, *Angew. Chem. Int. Ed*., 2019, **58**, 2284 – 2288.